Evaluating the Impact of Non-Linear Contact Modeling in Connecting Rod Durability Analysis.

M. H. Rahmat, A.N. Mahmood Zuhdi and S.H. Ismail

PETRONAS Research Sdn Bhd, Bangi, Malaysia

The immense reciprocating energy transfer in a connecting rod leads to durability concerns in an automotive engine design. The resulting cyclical compressive and tensile stresses derive from the dynamics initiated by the mass inertial forces, the combustion compressive forces, and the resulting reaction forces. Three vital components to this analysis are the effective pressure in the cylinder, crankshaft dynamics and the connecting rod dynamics. Using validated data of effective combustion pressure and the corresponding crankshaft dynamics, the connecting rod load dynamics were obtained. These loads are robustly interacting with the connecting rod through the contact of journals and bearings.

Simulation performed using the non-linear contact distribution would obtain insights into the structural integrity and the durability of the connecting rod. A comparison of the classical, linear and non-linear contact quasi-static finite element methods will provide distinguishable observations on the accuracy and costs of the respective methods in the connecting rod design process.

Keywords: Non-linear contact, Fatigue, Fatigue Life, Powertrain

1. Introduction

A connecting rod is the linking component between the piston and the crankshaft of the conventional internal combustion engine. It functions as the conversion mechanism for the transfer of heat energy from the combustion to the eventual mechanical work received by the crankshaft. Although the shank of the connecting rod is a simple mechanical component, there are other features of interest which are relatively complex geometrically. In reference to Figure 1, the components employed are the piston pin (a), small end bearing (b), connecting rod shank (c), connecting rod cap (d), big end bearing (e), bolts (f) and the crankshaft (g).

The structural integrity and durability of a power component like the connecting rod in a powertrain system during high load operating conditions are important design considerations (Ramachandra, 2006) (Chacon, 2006). Operational conditions impose mean stresses as well as cyclical stresses to the connecting rod's overall and detailed structure. Methods used can vary from purely classical calculations to non-linear analysis (Sobel,1979) (Peixoto, 2004). Determining the most physical but least expensive methodology is essential to obtain accurate results within reasonable cost. The results obtained allow engine design engineers to evaluate the connecting rod durability and assist in powertrain design optimization.

Automotive design engineers require quick but reliable analysis to support their respective design concepts and projects. Determining the most physical but least expensive methodology is essential to obtain accurate results within reasonable cost. The results assist automotive design engineers to evaluate the connecting rod durability and assist in powertrain design optimization.

Many engineers resort to the over-simplistic rule-of-thumb to support their design decisions before employing other considerations. The most simplified yet valid physical variety would be through lookout tables for established design conditions and physics. These are procured from experimental readings comparable to steam properties tables and airfoil aerodynamic profile table. This is followed by the zero-dimension engineering models, one-dimensional approximated physical models and up to the fully three-dimensional physical models, with complexity increasing as shown in Figure 2.

As the complexity of the problem increases, more computing power is required to obtain the necessary results. Increasingly complex physical model introduces additional non-linearity, as physical models are predominantly non-linear in nature. In the less complex models, the non-linearities are commonly pseudo-linearised to help engineers to speed up quantitative calculations, assuming reasonable numerical mathematics was subsequently employed.

In the present article, the calculation and computation involve the quantification of connecting rod durability using three methods, namely the classical design methodology, the linear finite element static stress analysis and the non-linear contact finite element static stress analysis. Fundamentally, there are other methods that could be used, but these three represent the most simplified, the simplified physical application and the physically more realistic methodology.

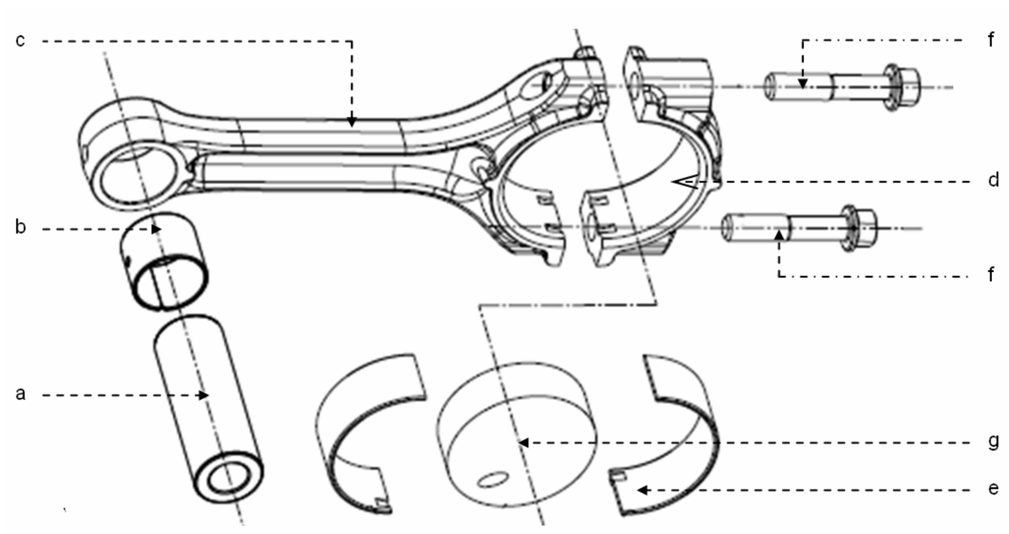

Figure 1. Nomenclature of a connecting rod

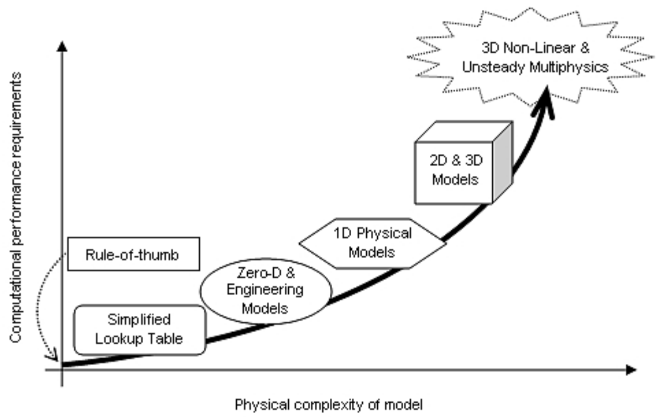

Figure 2. Physical complexity and CPU performance.

Finite element structural analysis had been the basis of structural integrity investigations common to today's engineering structural analysis practice. The most basic form of analysis is the linear static problem which gives the analysts approximated insights on stress distribution and structural deformation based on the manipulation of the elastic material properties, element displacements and stresses obtained through Hooke's Law. This method has been found reliable and accurate and sufficient for linear structures, with minor approximation and discretisation errors.

However, since all physical things are naturally non-linear, it is better to model some part, if not all, of the non-linear functions. There are three fundamental categories of non-linear computations (Nicholson, 2003) (Cook, 1995), namely the material non-linearity (Ligier, 2006), geometric non-linearity and the boundary condition non-linearity. Material non-linearity can occur through the non-linear dependence of the stress on the strain or temperature. Geometrical non-linearity occurs due to large deformation, thus making strain measurement necessary as the stress conjugates to it. Finally, there is the boundary condition non-linearity that occurs due to the non-linearity of the support boundary or contact.

For the current non-linear analysis approach, the boundary condition non-linearity is employed. The boundary condition involved is the contact non-linearity on the adjoining surfaces of the connecting rod.

2. Connecting Rod Durability Analysis

A comparison between three different approaches is performed to obtain the comparative connecting rod durability. The first approach is the classical stress calculation method that applies the simplified approximation of the stresses and loads in a connecting rod. In addition, a computational structural dynamics simulation is performed by the finite element method. The computational method would be segregated into the linear analysis and the non-linear contact analysis. Thus, all three methods will be used to obtain the required results.

It is particularly important to focus on the important aspects of the relatively complex connecting rod component geometry. The general fatigue safety factor of the overall connecting rod, connecting rod shank and the cap fillet region is the features of interest. Additionally, the bearing geometry deformation is equally important to comprehend the effects of bearing surface contact non-linearity on the differences in the results.

2.1 Connecting rod configuration and load cases

Investigation on the durability of the connecting rod covers multiple important engine speeds (Chacon, 2006). This investigation applies the engine speeds which signify the speed representing the maximum torque (T_{max}), maximum power (P_{max}) and the instantaneous engine over-speed ($\omega_{overspeed}$). The engine speed for the maximum torque indicates the maximum compressive forces acting on the piston from the combustion in the cylinder. This is thus transferred to the connecting rod, leading to high compressive stresses.

On the other hand, the engine speed signifying the maximum horsepower and instantaneous engine over-speed indicates the maximum inertial effect encountered by the connecting rod, especially at the top dead center non-firing. At this condition, the connecting rod is predictably strained furthest from the crankshaft due to the absence of compressive pressure to damp the tensile forces. For high speed gasoline engines, tensile stresses are dominant and thus the connecting rod is at its most vulnerable.

For each of the engine speed, eight load cases were specified to represent the rotating crankshaft's relation to the connecting rod. This is required to perform the quasi-static simulation, where a static run represents a system in motion, in this case the connecting rod sliding on a rotating crankshaft. The loads are applied on the piston pin, signifying the connection to the piston. The load cases can be categorised as the assembly load and the operating loads. The operating loads are obtained from the instantaneous condition at the maximum cylinder pressure, maximum compression on shank, top dead center non-firing and four maximum bending loads. These loads are obtained from the calculated engine dynamics shown in Figures 11, 12 and 13 in the appendix.

2.2 Classical Calculation

Classical calculations of a connecting rod revolve around the manipulation of stresses around simplified structures. These include simplified calculations of tensile stresses, compressive stresses, bending stresses and hoop stresses. Engineers frequently apply these calculation methods when given a structural integrity problem.

For a shank component of the connecting rod, the stresses obtained are calculated by using the connecting rod properties (connecting rod assembly mass, shank's area, shank's second moment of area), the material properties (compressive yield strength, Young's Modulus, ultimate tensile strength, fatigue strength) and the engine properties (bore, stroke, engine speed, crank throw, piston assembly mass). The fatigue strength is obtained by applying the ultimate tensile strength, fatigue stiffness, and manufacturing process factor into the empirical equation

$$\sigma_f = 0.425 \cdot \sigma_{UTS} \cdot K_f \cdot F_m$$

The alternating stress is obtained by taking the average of the maximum compressive stress and the maximum tensile stress. Thus, the mean stress is obtained by subtracting the alternating stress from the maximum tensile stress.

$$\sigma_{alt} = \frac{\sigma_{comp} + \sigma_{tens}}{2}$$

$$\sigma_{mean} = \sigma_{tens} - \sigma_{alt}$$

Thus, the Goodman fatigue safety factor could be obtained by the following equation:

$$FSF_{Goodman} = \frac{\sigma_f}{\sigma_{alt}\left(\frac{\sigma_{UTS} - \sigma_{mean}}{\sigma_{UTS}}\right)}$$

2.3 Alternative Goodman fatigue safety factor

Quantifying the durability of any structural dynamics, the alternative Goodman general fatigue safety factor calculation is applied. The fatigue safety factor is calculated on the surface of the connecting rod to indicate the location of crack initiation. The results are processed by using certain factors to model the effects of manufacturing processes used in the construction of the connecting rod. The processes involved are forging, grinding and machining. The surface finish affects the stress values on the surface of the connecting rod, thus providing empirically accurate values to the fatigue safety factor.

The alternative Goodman is the improvement of the Goodman method for calculating fatigue safety factors. Safety factor calculations are important indications of the durability of the structural component. Applying the mean stress and the alternating stress, the alternative Goodman general fatigue safety factor is obtained by geometrically plotting the stress point and material property lines on the Goodman diagram, and taking the scale as shown in Figure 3. Alternatively, the scale can be calculated from trigonometry and consequently calculating the fatigue safety factor by the scale of the origin-point distance over the origin-safety line. In relation to Figure 3, the fatigue safety factor equation is

$$Fatigue\,Safety\,Factor = \frac{r_a + r_b}{r_a}$$

The Goodman diagram is built from three lines constructed from the ultimate tensile stress (σ_{ut}), tensile yield stress (σ_{yt}), compressive yield stress (σ_{yc}) and the fatigue limit stress (σ_{fl}). In summary, if the point is located in the grey region, the component's durability is considered good. The fatigue safety factor is an indication of operational safety of the component.

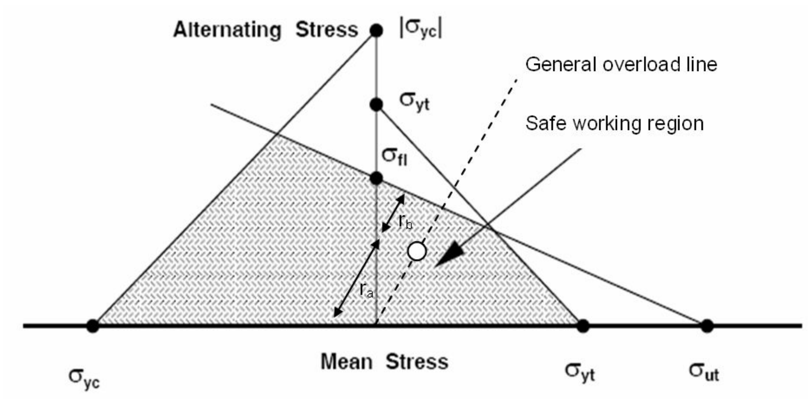

Figure 3. Goodman diagram

3. Structural Simulation Strategy

3.1 Spatial discretisation and loading strategy

The connecting rod geometry must first be spatially discretised before it could be used in any finite element software. The connecting rod is discretised mainly into tetrahedral elements while the bolts and bearings have pentahedral elements due to its thin and simplified nature. In general, non-critical regions are discretised using coarser elements, as seen in Figure 4. For the geometrically detailed and critical regions, finer elements were used to increase geometrical accuracy and to enhance the stress fidelity. Among other critical regions, the cap fillet discretisation is enclosed in the dotted circle in Figure 4b.

The discretisation is segregated into the respective components. This is to model different components as they physically exist. Once the discretisation is completed, the loads have to be applied to the piston pin front and rear portion. This replicates the load transmission of the piston to the pin, and thus ultimately to the connecting rod.

The loading is generated by the computation of rigid engine dynamic system for all the load cases, which calculates the dynamics of the crankshaft, connecting rod, piston and combustion chamber pressure. The resulting loads for each load case are given as the magnitude and vector on a particular node on the piston pin. Therefore, a distribution of loads is obtained on the piston pin surface (Figure 5) for every quasi-static load case. The calculation of the loading is based on the effective pressure of the cylinder, position of the crank and the engine speed at the previously referred load cases. The data for the engine dynamics could be observed in the appendix.

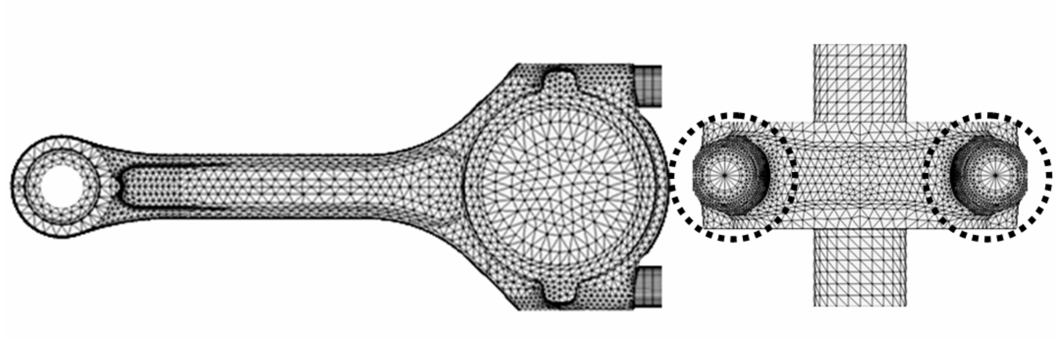

Figure 4. Spatially discretised connecting rod. a) Side b) Bottom

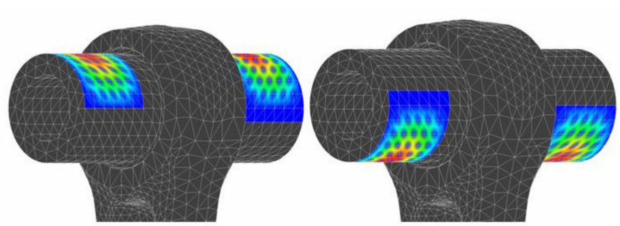

Figure 5. Piston pin load distribution

3.2 Quasi-static linear and non-linear contact finite element analysis

A quasi-static finite element analysis applies static computation at different temporal instances which simplifies an unsteady system to a steady reciprocating system. Therefore, the computation is simplified because the computations performed are only static computations. The distribution of static load cases is set based on the predetermined assembly and operational load cases.

Linear finite element analysis employs only linear modeling of the connecting rod elements. Fundamentally, it applies the processing of the force matrix and the deformation matrix $(\bar{F} = k\bar{x})$ based on the linear stiffness of the elements. The stresses are then calculated by means of the Hooke's Law in relation to the stress and strain values $(\sigma = E\varepsilon)$. Fundamentally, the nodes are modeled to be in continuum and are elastically connected between contact surfaces.

Non-linear contact simulation is similar to the linear finite element analysis except that it models all the contacting parts in a segregated manner, where the deformation will effect the respective load distribution, and vice-versa. Although each parts are still respectively elastic in nature, the contact surfaces are not linked to each other, except for the incident of contact and independent transfer of forces to achieve dynamic equilibrium.

3.3 Constraints and contacting surfaces

Setting restraints to a model of a discretised structure is necessary to prevent the model from becoming singular, thus unsolvable. At the same time, the prospect of over-restraining the model must not be overlooked. Thus, it is recommended to restrain it using the 3-2-1 method for a static computation. The crank cross-section is constrained in X-Y-Z direction, some nodes on the pin cross-section are constrained in X-Z direction and the shank is constrained with an imaginary spring on the X direction. The crank X-Y-Z constraint holds the connecting rod in its position on the coordinate system and eliminates the axial degree of freedoms. X-Y and X constraint eliminates the rotational degrees of freedom.

In addition to the restraints, congruent connecting surfaces are paired into respective sets to apply joined boundary condition for linear simulation and a more physical contact pair modeling for the non-linear simulation. In the linear computation, selective node pair joins were used to constraint the respective pairs for all 6 degrees of freedom. In order to apply these constraints, the meshes must be geometrically congruent to the respective contacting sides.

The non-linear contact finite element analysis utilizes the small sliding contact modeling with surface-to-surface tracking approach. Small sliding assumes relatively minimal sliding of one surface along the other, thus is suitable for this simulation. Surface-to-surface tracking is used because the contact is averaged across the surface between related nodes. This eliminates large undetected penetration of master nodes into the slave surfaces. The properties of the surfaces would be elastic and deform according to the forces applied to it, which in turn conjugate with the opposite surface. This conjugation requires iterations to obtain a converged value and the converge profile of the connecting rod static analysis. Essentially, the adjoining contacting surface pairings applied are as listed in Table 1.

Non-linear Contact pairing	**Master Surface**	**Slave Surface**
Pin to Small end bush	Bush	Pin
Small end bush to shank	Shank	Bush
Shank to cap	Shank	Cap
Rod to big end bearing	Rod	Bearing
Big end bearing to crankshaft	Bearing	Crankshaft
Contact Constraints	**Type**	
Cap to bolt	Constrained node pairing	
Bolt to shank	Constrained node pairing	

Table 1. List of adjoining surfaces

4. Durability Calculation and Simulation Results

4.1 Connecting rod shank fatigue safety factor distribution

When the computation is done and post-processed, the connecting rod simulation results can be observed in Figure 6. The colour spectrum is equally scaled from 1.7 (red) to 2.5 (blue) for all cases to produce comparative representation. Obviously, Figure 6 shows that the linear quasi-static finite element analysis demonstrates an optimistic fatigue safety factor (FSF) distribution throughout. However, the main shank regions show modest differences due to the uniform axial geometry which is located at a sufficient distance away from the contact model region of influence. The largest variation in the FSF distribution occurs when the shank transforms into the big end. At this region, the non-linear contact FSF is lower than the linear counterpart, thus has lower durability.

On the other hand, at the instantaneous engine over-speed, the FSF at the shank is higher than 2.5 for both the analysis methods. The smaller difference between the tensile forces from the inertia and compressive forces during combustion at the instantaneous engine over-speed results in reduced alternating stress, thus presenting higher durability for axially loaded components.

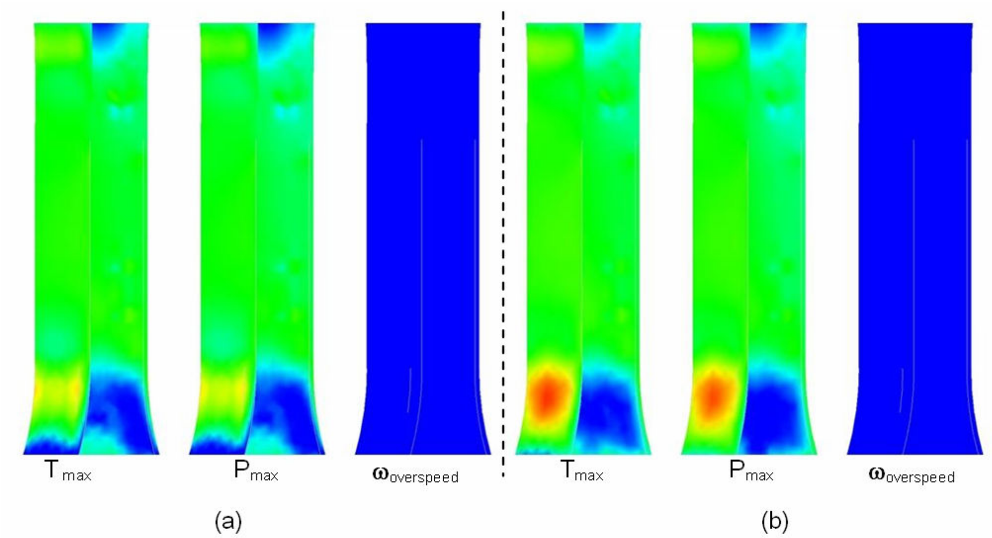

Figure 6. Shank fatigue safety factor distribution a) linear b) non-linear

4.2 Cap fillet fatigue safety factor distribution

At the cap fillet as seen in Figure 7, a more explicit demonstration of the differences between linear and non-linear contact is established with a similar scale of 1.7 (red) to 3 (blue). Figure 7a shows overall similarity of all three engine speed cases for the linear analysis; albeit minor variation. It gets increasingly interesting with the non-linear contact cases in Figure 7b, with more durability concerns appearing.

Evidently, the FSF decreases as the engine speed increases to the maximum value at the instantaneous engine over-speed. This shows that the cap fillet region is dominantly caused by the inertial forces of the connecting rod. The increase observed is greater for the non-linear contact analysis in comparison to the linear analysis. This shows that the difference in using linear and non-linear contact for a connecting rod is significant, providing curiosity to its accuracy and physical feasibility. Later, an observation on the comparative bearing deformation can demonstrate the effects of the non-linear contact in this investigation.

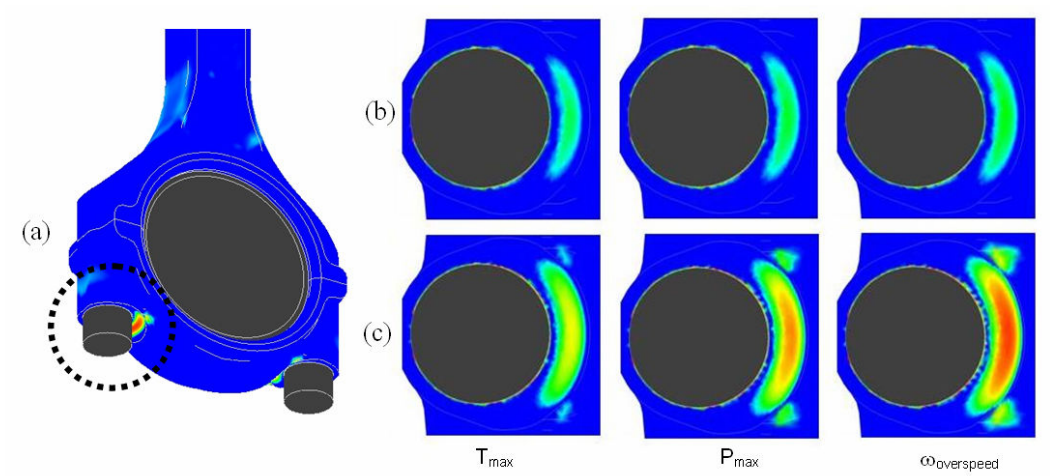

Figure 7. Cap fillet fatigue safety factor distribution a) cap fillet location b) linear c) non-linear

4.3 Collocated fatigue safety factor value comparison

Coloured spectrums of safety factor distributions demonstrate the qualitative comparison between the different engine speeds and analysis techniques. Quantitatively, we can obtain the collocated fatigue safety factor and compare to each respective analysis method. Table 2 shows the fatigue safety factor values of two exact nodes representing the connecting rod shank and the cap fillet.

Noticeably, fatigue safety factor values for the linear analysis are higher than the non-linear contact analysis for every engine speed and region observed. This demonstrates that the linear analysis is more optimistic in nature compared to the non-linear contact analysis.

	Component	Engine Speed	Classical calculation	Linear FEA	Non-Linear Contact FEA
Fatigue Safety Factor	Conrod Shank FSF	T_{max}	1.526	2.094	2.076
		P_{max}	1.708	2.109	2.086
		ω_{max}	5.741	3.252	3.242
	Cap Fillet	T_{max}	Not Available	2.371	1.904
		P_{max}	Not Available	2.312	1.729
		ω_{max}	Not Available	2.268	1.619

Table 2. Comparison of maximum fatigue safety factor values.

4.4 Bearing deformation observation

The variation of the FSF distribution featured in the shank and cap fillet region can be reasonably rationalized through the observations of the deformation encountered by the big end bearing (Merritt, 2004) (Mian, 2002) (Peixoto, 2004). Since the contact applied would give different

axial

contact force distribution, it iteratively transforms the deformation according to the elasticity of the material. The pre-deformed geometry of the big end bearing could be observed in Figure 8.

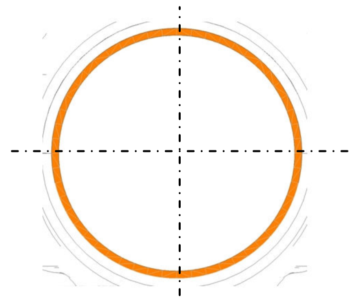

Figure 8. Big end bearing before deformation

4.5 Big end bearing deformation

The big end bearing deformations are displayed in Figure 9 and Figure 10 under the maximum cylinder pressure load and the top dead center non-firing load, which coincide with the 17^0 and 360^0 crank angles respectively. These coincide with the largest compressive and tensile force applied to the connecting rod. The deformations observed have been scaled to a factor of 100 in all cases for both analyses.

The deformation for the linear analysis (a) could be observed to be perfectly rounded for both load cases. However, it is actually physically inappropriate and inaccurate. The bearing seems to unnecessarily augment without reason to follow its connected node on the rod surface. This proves that the linear analysis is not physical when there is an occurrence of contact.

On the other hand, the non-linear contact reveals that the bearing conforms to logical physical representation. The bearing does not augment nor is it forced to clinch to the neighboring node without properly applied dynamics. At maximum cylinder pressure, the bearing is axially compressed and at 360^0 crank angle is laterally compressed by the deforming shank and cap under tensile exertion.

These deformations would introduce a varying force application on the respective nodes, which is not necessarily moving together. Therefore, it can be assumed that the non-linear contact ensures a more realistic physical similitude.

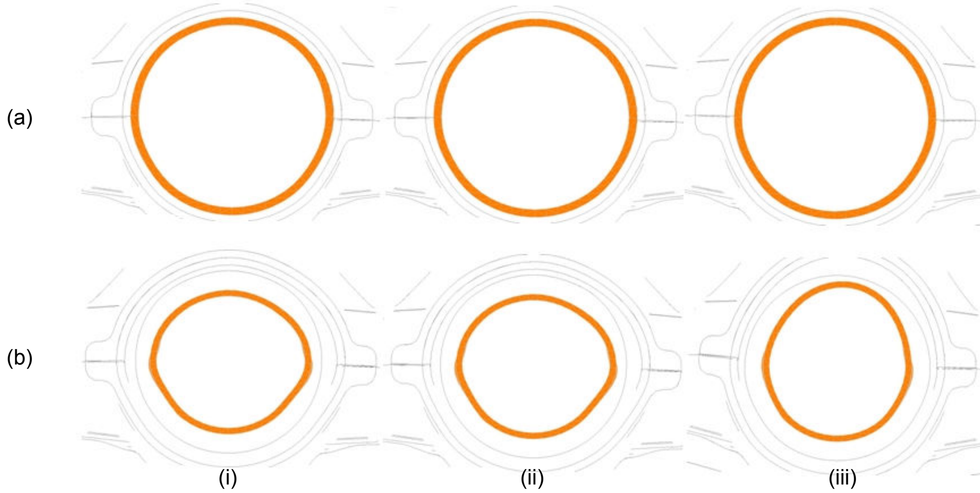

Figure 9. Maximum cylinder pressure small end bearing deformation a) linear b) non-linear i) T_{max} ii) P_{max} iii) ω_{max}

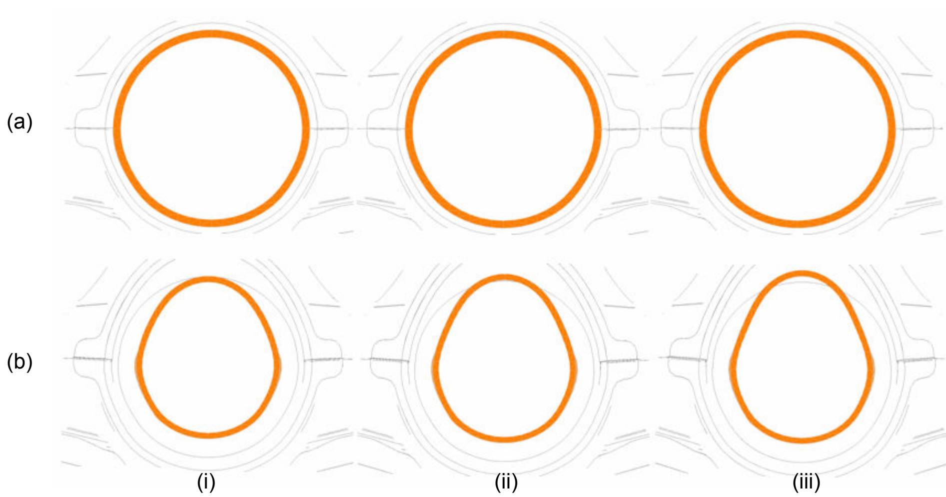

Figure 10. Top dead center non-firing big end bearing deformation a) linear b) non-linear i) T_{max} ii) P_{max} iii) ω_{max}

5. Conclusion

In comparison, classical calculations are the cheapest mode to obtain the fatigue safety factor. The non-linear contact is the most expensive since it requires multiple iterations compared to the solitary solution iteration for the linear analysis. In addition, the non-linear contact solution procedure has an extra algorithm to transiently shift the contacting surface geometry according to the forces conjugating on each of the master and slave surfaces.

Each of the three methods has its own advantages and disadvantages. The classical calculations would allow faster calculations but undesirable gross assumptions. The computational methods are superior in much challenging geometries, but additionally come with other academic assumptions. The linear computation is quicker but fails to physically model the non-linearity in the contact scenario for the connecting rod. The non-linear analysis better simulates this contact non-linearity but comes with a higher computation cost. The linear quasi-static finite element analysis gives a more optimistic computation of the fatigue safety factor, the inaccuracy of which would pose the possibility of durability concerns in operation.

In conclusion, the results from non-linear contact simulation appear more physically realistic compared to its linear counterpart under similar discretisation, geometry and loading. The classical calculations have low accuracy and dire fidelity but gives quick solutions. Understanding the advantages and limitation of these methods, both in accuracy and time, would allow automotive engineers to make adept judgment on the respective designs.

6. References

1. Chacon, H., “Structural and Fatigue Numerical Analysis for Connecting Rods Development”, SAE Technical Paper Series, 2006-01-2515, 2006.
2. Cook, R.D., “Finite Element Modeling for Stress Analysis”, John Wiley & Sons, Inc., 1995.
3. Ligier, J.L., “Circular Systems with Non Linear Stiffnesses”, SAE Technical Paper Series, 2006-01-1636, 2006.
4. Merritt, D., and Zhu, G., “The Prediction of Connecting Rod Fretting and Fretting Initiated Fatigue Fracture”, SAE Technical Paper Series, 2004-01-3015, 2004.
5. Mian, O., Merritt, D., Wang, D., “Numerical Simulation of the Profile Influence on the Conrod Bearings Performance”, SAE Technical Paper Series, 2002-01-0295, 2002
6. Nicholson,, D.W., “Finite Element Analysis, Thermomechanics of solids”, CRC press, 2003.
7. Peixoto, V.J.M., Zottin, W., “Numerical Simulation of the Profile Influence on the Conrod Bearings Performance”, SAE Technical Paper Series, 2004-01-0600, 2004
8. Ramachandra, P., Yeongching, L., Yasuhara, J., Hayama, K., “Durability of Power Components under Operating Conditions”, SAE Technical Paper Series, 2006-01-0650, 2006
9. SIMULIA, “Abaqus – Analysis User’s Manual”, Dassault Systemes, 2008
10. SIMULIA, “Abaqus – Theory Manual”, Dassault Systemes, 2008

7. Appendices

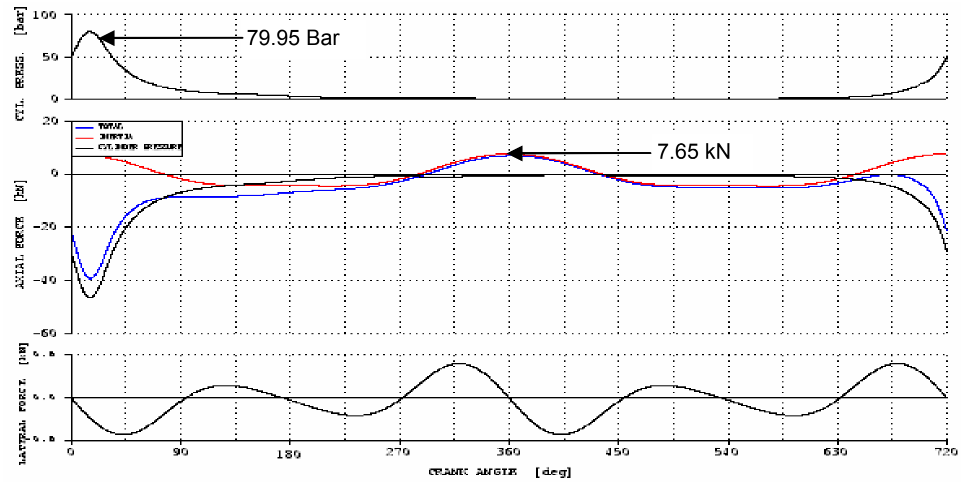

Figure 11. Engine dynamics at maximum torque incidence

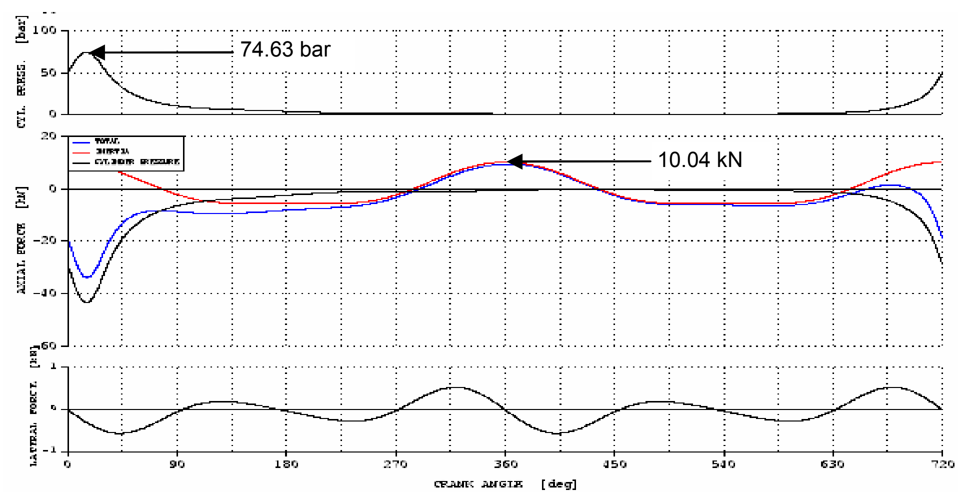

Figure 12. Engine dynamics at maximum power incidence

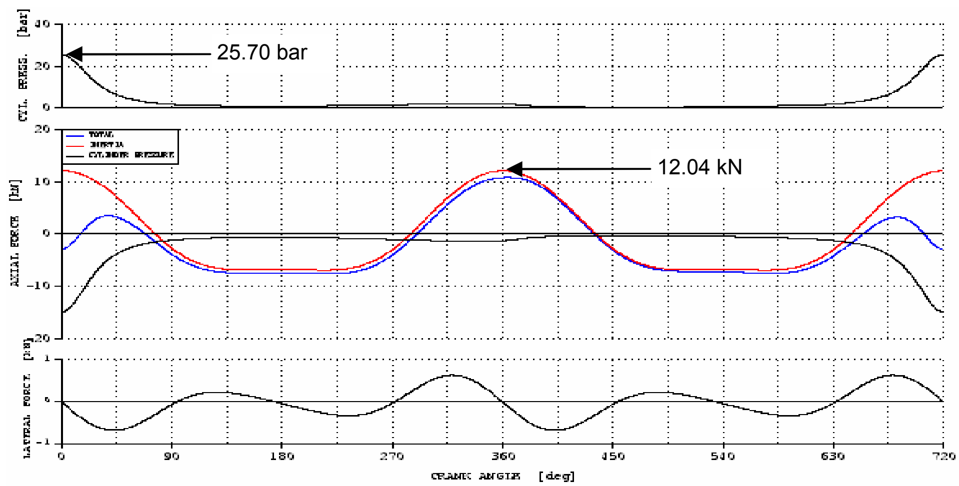

Figure 13. Engine dynamics at instantaneous overspeed

8. Acknowledgement

We would like to extend my deepest gratitude to PETRONAS and PETRONAS Research Sdn Bhd for the permission to reproduce the data used in this paper.